Intersubband spectroscopy and valley degeneracy of Si(110) and Si(111) *n*-type inversion layers

T. Cole
Michelson Laboratory, Naval Weapons Center, China Lake, California 93555

B. D. McCombe
Department of Physics and Astronomy, State University of New York at Buffalo, Buffalo, New York 14260 and Naval Research Laboratory, Washington, D.C. 20375*

(Received 12 September 1983)

Detailed far-infrared frequency domain intersubband spectroscopy has been carried out on Si(110) and Si(111) *n*-type inversion layers at 4.2 K. Studies of the polarization dependence of the spectra of the (110) samples are consistent with a fourfold valley degeneracy for these samples and with recent calculations of Yi and Quinn. However, measured transition energies are consistently lower than those calculated. Both normally processed and specially Ar-annealed (111) samples were investigated. Normally processed samples exhibited twofold valley degeneracy as determined by Shubnikov—de Haas measurements, and polarization dependences were again in good agreement with the calculations for twofold degeneracy. However, transition energies were substantially lower than those calculated. Ar-annealed samples were found to have a valley degeneracy of 6, in agreement with previous work. Transition energies for these samples were 9—10 meV below those for the twofold samples, and very small shifts to higher energy were observed for the infrared electric field polarized perpendicular to the interface compared with the parallel polarization. The apparent disagreement of the latter result with calculations appears to be due to the lack of substantial depletion charge in the perpendicular polarization samples. The large discrepancy in transition energies for these samples is attributed in part to interface degradation. The (111) optical results are internally consistent with built-in stress or built-in stress modified by many-body effects as the underlying mechanism producing the twofold valley degeneracy; however, the present results do not establish this unambiguously.

I. INTRODUCTION

Electron space-charge layers on the (110) and (111) surfaces of Si are neither as completely studied nor as well understood as those for Si(100). For both former surfaces, experimentally determined valley degeneracies and effective masses have been reported that are different from those predicted by effective-mass theory.[1] A study of the intersubband transitions is expected to provide complementary information to that contained in transport and magnetotransport measurements and thus help to improve our understanding of the electronic properties of these surfaces.

Far-infrared Fourier-transform spectroscopy has proven to be a useful tool for studying the intersubband transitions of carriers in space-charge layers on metal-oxide-semiconductor structures.[2] The intersubband transition energies are sensitive to many-body effects which are important in determining the energetics and dynamics of the two-dimensional electron gas forming the inversion layer.[3] In this paper, we present results on inversion layers on the (110) and (111) surfaces of Si and discuss them in terms of current theoretical models, some of which were proposed to explain other experimental observations.

In the following sections we present a brief discussion of the (110) and (111) surfaces which provides a rationale for the current interest and serves to motivate the present study. Next, a short description of the salient features determining the subband energies and intersubband transition energies is presented. A brief discussion of the experimental technique is followed by the experimental results and a discussion of the significance of these results in terms of the various theoretical models that have been advanced to date, with particular emphasis on the recent work of Yi and Quinn.[4]

II. BACKGROUND AND MODELS

Si has six conduction-band minima located along the ⟨100⟩ directions which project onto the (111) surface to give six equivalent valleys, 12 with spin included (see Fig. 1). In the independent-particle effective-mass approximation, the surface electric field does not remove this degeneracy (since the effective mass perpendicular to the interface is the same for all ellipsoids), and a sixfold valley degeneracy is expected. However, a number of magnetotransport measurements[5] have found a valley degeneracy of 2 for *all* principal surfaces of Si. Later experiments by Tsui and Kaminsky[6] demonstrated that the valley degeneracy for the (111) surface, obtained in the above manner, depends on the processing steps used to prepare the samples; valley degeneracies of both 2 and 6 have now been obtained by a number of workers.

For the (110) surface of silicon the six conduction-band

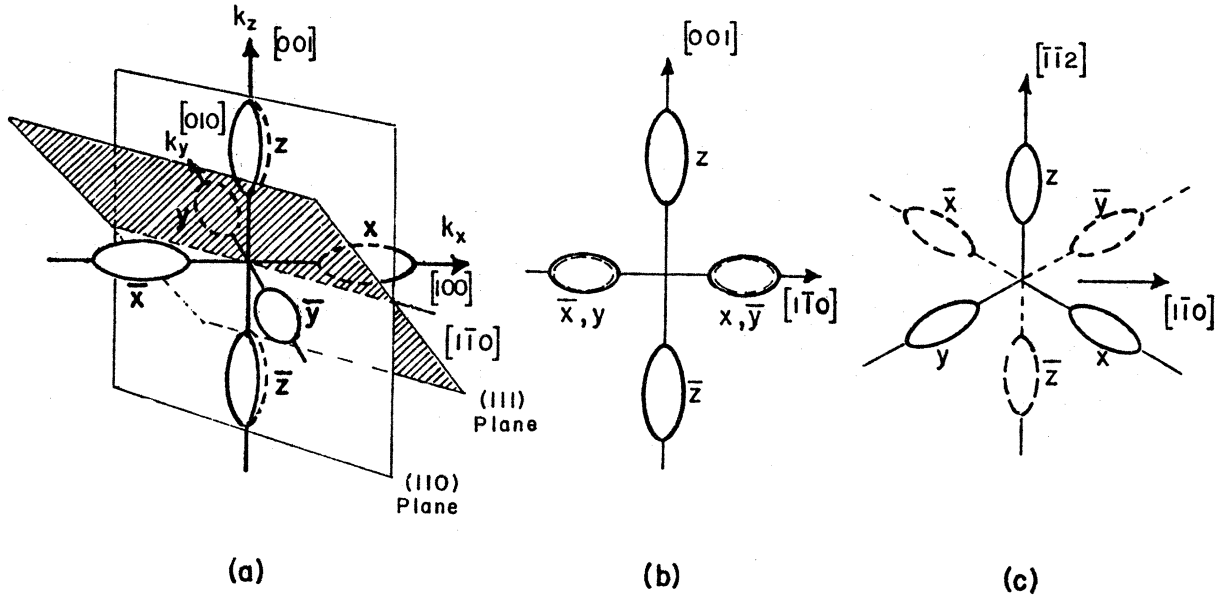

FIG. 1. (a) Schematic diagram of constant-energy surfaces for Si. (110) and (111) planes are indicated. (b) Projection of the constant-energy surfaces onto the (110) plane. Dashed curves represent surfaces $(\bar{x},\bar{y})$ originating behind the plane. (c) Projection of the constant-energy surfaces onto the (111) plane. Dashed curves represent surfaces ($\bar{x}$, $\bar{y}$, and $\bar{z}$) originating behind the plane.

minima in the presence of the surface electric field give rise to four degenerate valleys, eight with spin, which are lowest in energy, and two degenerate valleys, four with spin, somewhat higher in energy. Again, early transport experiments[5] also gave a valley degeneracy of 2 for this surface. However, more recent experiments have shown that in samples having undergone normal processing the valley degeneracy is 4 and the spin degeneracy is lifted at the magnetic fields at which the experiments are performed.[7] Thus, it now appears that the perplexing problems concerned with the anomalous valley degeneracy are confined to the (111) surface alone.

Several models have been proposed to explain the anomalous valley degeneracies observed in these surfaces. The most straightforward of these[6,8] makes recourse to large, local, inhomogeneous stresses at the oxide-semiconductor interface as the cause of the lower degeneracy observed in some samples. In this model, the large stress splits the sixfold degeneracy, lowering two of the valleys substantially below the other four. On the other hand, other workers[9] have concluded from measurements of mobility anisotropy and Shubnikov–de Haas oscillations that such large stresses are unlikely. They argued that such a large splitting implied much larger stresses than were applied in their experiments, while the mobility anisotropy measurements indicated that the local inhomogeneous stresses and the applied stress were of the same order.

Two possible means of resolving this dilemma have been proposed. The first of these is based solely on many-body effects.[10] Simply stated, the argument is that the ground occupied state (lowest subband) is lowered due to exchange and correlation, and the amount of lowering is proportional to the Fermi energy at constant electron density ($E_F \propto n_s / g_s g_v$, with g_v denoting degeneracy, g_s denoting spin degeneracy, and n_s denoting surface electron density). A transition to a lower-degeneracy ground state can become favorable at densities low enough that the energy lowering due to many-body effects is greater than the corresponding gain in kinetic energy. However, this effect is much too small[11] ($\sim$1–2 meV) to account for large valley splittings. Very recent theoretical work[12] at finite temperatures has emphasized that the self-energy corrections are only weakly dependent on surface orientation and valley degeneracy. Bloss *et al.*[11] have suggested that this effect may be enhanced by relatively small amounts of inhomogeneous stress on the (111) surface to the extent that the transition takes place at somewhat higher carrier densities. They estimate that with exchange effects included, only about one-third as much stress is required to explain the apparent splitting between valleys.

Another model that accounts for the observed "valley degeneracies" without the need for large amounts of stress has been proposed by Vinter and Overhauser.[13] They suggest that the valley degeneracy deduced from the period of the Shubnikov–de Haas oscillations can be 2, even when the valleys are split only slightly in energy, provided that the stress splits the valleys into three pairs, and that the splitting is more than the width of the levels. This implies that all samples are "nearly" sixfold degenerate. Their argument is based on the assertion that the *Fermi energy* for the two-dimensional (2D) electron gas is not constant, but rather the *electron density* in the layer is constant for a given gate voltage. Hence, for sharp Landau levels, the Fermi energy is locked to the highest occupied Landau level and jumps to the next available Landau level when it is filled. The minima in the Shubnikov–de Haas oscillations occur whenever a Landau level is exactly filled; thus, the period in n_s (presumably directly related to the gate-voltage change through the device capacitance) is charac-

teristic of a valley degeneracy of 2 since each 2D Landau level holds $2g_v(eB/ch)$ electrons, and $g_v=2$ in this model. When there is substantial overlap of the broadened Landau levels from the three pairs of valleys, the measured g_v from the period will be 6. Since the Landau levels are relatively broad for the (111) and (110) samples (maximum mobilities of <2500 cm^2/V sec), it is expected that unless the splittings are actually quite *large* (in which case there is no difference between this model and that of Ref. 8), there should be some component of the sixfold-degenerate period in the measurements on "twofold" samples. Careful studies by two groups[14] have failed to reveal this feature and substantiate the fact that there are actually twofold- and sixfold-degenerate samples. In the twofold-degenerate samples, the energy splitting must be greater than the Fermi energy at zero magnetic field over the range of n_s studied.

An additional mechanism proposed to account for the lifting of the valley degeneracy is the occurrence of a charge-density-wave (CDW) ground state.[15] For example, intervalley exchange interactions between pairs of valleys can cause two valleys to be lowered relative to the other four in (111) inversion layers (thus a twofold-degenerate ground state). For Si(111), two kinds of CDW's have been suggested: a β CDW, in which two pairs of valleys interact and two valleys remain unaffected,[15] and a triple CDW, in which all three pairs of valleys interact.[16] The triple CDW is thought to be lowest in energy but unstable in the presence of even small amounts of stress.[17] For (110) layers, the same mechanism should be operable but with only one type of CDW, the one coupling pairs of valleys. A major objection to the CDW model is that the magnitude of the intervalley exchange interaction needed to explain the energy splitting among the valleys is considerably larger than that estimated for bulk Si.[18] A second difficulty lies in the reconcilation of this model with the fact that the experimentally determined degeneracy depends on the processing of the samples.

The sensitivity of subband spectroscopy to valley degeneracy and the motivation of the present work can be understood from the following qualitative arguments. The subband energies of charge carriers confined in a narrow region in the semiconductor near the oxide-semiconductor interface of a metal-oxide-semiconductor (MOS) structure depend on a number of factors. In addition to the depletion potential, image forces due to the presence of the oxide, self-consistency, and many-body effects (exchange and correlation) must be taken into account. The effective potential for a single quasiparticle may be written[3] as

$$V_{\text{eff}}=V_{\text{depl}}+V_{\text{image}}+V_{\text{Hartree}}+V_{\text{ex-c}}\ . \tag{1}$$

For space-charge layers in Si, the many-body effects have been shown to be large and very important in determining the subband energies.[3] Many-body effects, in particular exchange effects, depend on the Fermi energy, and thus will be different for different valley degeneracies as mentioned above. The larger the valley degeneracy, the smaller the Fermi energy at constant electron density. A smaller Fermi energy leads to a concomitantly smaller exchange lowering of the ground state and a smaller difference in energy between ground and excited states (since for the unoccupied excited states exchange effects do not contribute to the energy). Thus, at the same electron density, the subband separations are expected to be smaller for a sixfold-degenerate system than for a twofold-degenerate system.

In the presence of the external radiation needed to excite transitions between subbands, two additional effects must be taken into account. These are the so-called depolarization shift[19,20] and final-state interaction (or exciton-like effect).[21] The first of these, the depolarization effect, can be understood classically. It is a shift in the resonance position to energies higher than the subband separation due to the fact that the space-charge layer is a thin polarizable medium, and the electrons respond dynamically to the *internal* infrared electric field, not the applied field. For a two-level system [ground state ($i=0$) and one excited state ($i=1$)], the resonance occurs at a frequency[20,21]

$$\omega_{\text{res}}=\omega_{01}(1+\alpha)^{1/2}\ , \tag{2}$$

where α is proportional to the product of n_s and the oscillator strength of the transition, and ω_{01} is the frequency separation of the ground and excited state.

The final-state interaction is strictly a quantum-mechanical, many-body effect resulting from the Coulomb interaction of the optically excited electron with the hole left behind in the Fermi sea in the ground subband. This is a negative (attractive) correction that lowers the transition energy. Again, for a two-level system, it has been shown[21] that the resonance frequency including *both* effects can be written

$$\omega_{\text{res}}=\omega_{01}(1+\alpha-\beta)^{1/2}\ , \tag{3}$$

where β is a parameter that characterizes the final-state interaction. Ando[21] has also shown that for Si(100), α and β are nearly equal over a range of electron densities, and $\omega_{\text{res}}\approx\omega_{01}$. This near cancellation has been verified by other calculations.[22,23] For a multilevel system, in the absence of such near cancellation, there is a coupling among the various transitions and a concomitant shift in frequency and intensity of the individual transitions.

An additional complication (and benefit from the point of view of the present study) is present in the study of the (111) and (110) surfaces. Since the ellipsoidal constant-energy surfaces of the Si conduction band are tilted relative to these surfaces, intersubband transitions can be excited, in general, by radiation polarized *either* parallel or perpendicular to the interface since the mass tensors have off-diagonal components, and an infrared electric field in the plane can couple to motion perpendicular to the plane. When the principal axes of ellipsoids of constant energy are parallel or perpendicular to the interface, as for the (100) surface, subband transitions can be excited only by radiation polarized perpendicular to the interface. The depolarization shift depends on the polarization of the exciting light; thus, there can be relative shifts in the intersubband transition energies for polarizations parallel or perpendicular to the interface which complicate interpretation. On the other hand, these shifts also provide direct information about the valley degeneracy. Nakayama[16] has calculated the depolarization shifts for both polarizations for several models of the (111) surface, but has not includ-

ed vertex corrections. Ando, Eda, and Nakayama[24] have calculated the effect of the polarization on the absorption, and show that for light polarized in the (111) or (110) plane, the depolarization shift vanishes and the vertex corrections are reduced when the degeneracy is 6 and 4, respectively. The recent work of Yi and Quinn[4] is the most complete treatment to date, and provides a basis for detailed comparison with the present experimental results. These authors have calculated the subband energies, transition energies, and the polarization dependence of the latter for twofold and sixfold valley degeneracies on (111) and twofold and fourfold valley degeneracies on (110), including the anisotropy of the valleys and both depolarization and final-state interactions.

III. EXPERIMENTAL

The devices used in these studies were large-area (2.5×2.5 mm^2) metal-oxide-semiconductor field-effect transistors (MOSFET's) fabricated on (111) and (110) p-type substrates. Magnetotransport measurements to determine the valley degeneracy were done on small Hall-geometry devices that were fabricated on the same chips as the large-area devices. The sample properties are summarized in Table I. Most samples were processed with a standard procedure which includes a 30-min anneal in N_2 at 1000 °C after the gate oxidation. Some of the (111) samples were additionally annealed in Ar for 30 min before and after the gate oxidation.

Two sets of (111) samples were fabricated. The first of these (sample 4) had 2900-Å-thick gate oxides, thick-Al-gate metallization, and no backside diffusion. Measured peak mobilities (from conductance-voltage curves at 4.2 K) were ~2500 cm^2/V sec. A degeneracy of $g_s g_v = 4$ was determined from magnetoconductance oscillations at 4.2 K in the usual manner. More careful studies of the Shubnikov–de Haas oscillations on samples from this same wafer by Woo and Stiles[7] indicate that the valley degeneracy g_v is indeed 2 and not 6. One set of the remaining (111) samples (samples 5 and 6) with 2000-Å-thick oxides (which had boron diffused into the backside) had an equilibrium depletion charge of $1-2\times10^{11}$ cm^{-2}. These wafers were fabricated both with thick gold on chromium and with semitransparent [(50–100)-Å] chromium gates. Peak mobilities at 4.2 K for these devices were measured to be $\lesssim1000$ cm^2/V sec, and the measured valley degeneracy was 6. The final set of (111) samples (samples 7 and 8) was fabricated on 1000-Ω cm p-type Si wafers with a 2200-Å-thick oxide. The equilibrium depletion charge for these samples (from the acceptor doping density) is $\sim1.5\times10^{10}$ cm^{-2}. Both thick- and thin-gate devices were made with "normal-" and Ar-annealing and diffused-boron backside contacts. The peak effective mobilities at 4.2 K were very low for both sets of samples (see Table I).

Two separate processing runs for (110) samples were carried out. The processing was the same as for the normal (111) samples except for the backside doping. In the first set of samples (sample 1), boron was diffused into the backside. These samples had peak effective mobilities at 4.2 K of 2000 cm^2/V sec. The equilibrium depletion charge could not be determined experimentally with any degree of confidence due to problems with the substrate contacts. In spite of this, these samples exhibited clear inversion line shapes with well separated 0-1 and 0-2 transitions indicating a depletion charge of nearly 10^{11} cm^{-2}, consistent with the substrate doping. A valley degeneracy of 4 was measured for these samples. The remaining (110) samples (samples 2 and 8) had boron ions implanted into the backside. The mobility of these samples was typically 800 cm^2/V sec, and the equilibrium depletion charge was determined to be $2-3\times10^{11}$ cm^{-2} from the substrate bias dependence of the threshold voltage at 77 K. However, these samples exhibited quasiaccumulation behavior at 4.2 K. Samples with both thick- and thin-gate metallization were available.

The experiments were carried out with a far-infrared Fourier-transform spectrometer and light-pipe system, as described previously.[2] The detector was a 4.2-K Ge:Ga photoconductor. In this work, light polarized perpendicular to the interface was obtained by mounting samples with thick metal gates on a 45° Si prism as in the previous studies. Samples with thick oxides and thick gates were mounted on the prism as above, and a linear polarizer ($>95\%$ polarization efficiency) was placed in the beam in front of the prism to polarize the incident light in the plane of the interface. With a 2900-Å-thick oxide, a small amount of parallel polarized light is coupled into the inversion layer in this geometry. Other samples with semitransparent gates were studied in the simple transmission geometry; i.e., with the (unpolarized) light incident normal to the sample surface which was mounted on a brass disk with a 3-mm central aperture. Si wedges were glued to

TABLE I. Sample properties.

Sample no.	Surface orientation	Annealing	Measured valley degeneracy (g_v)	Gate metallization	Oxide thickness T_{ox} (Å)	μ_{eff}(peak) (cm^2/V sec)	Threshold voltage V_T (V)
1	(110)	N_2	4	Cr-Au	2300	2000	0.05
2	(110)	N_2	4	Cr-Au	2000	800	−3.0
3	(110)	N_2	4	Cr	2000	800	−4.0
4	(111)	N_2	2	Al	2900	2500	0.5
5	(111)	Ar	6	Cr-Au	2000	1000	−4.0
6	(111)	Ar	6	Cr	2000	1100	−3.0
7	(111)	Ar		Cr	2200	500	−2.7
8	(111)	N_2		Cr	2200	950	−1.9

the backside of these samples to minimize multiple internal reflections.

In all cases with the spectrometer light source "on," the gate voltage of the device was square-wave-modulated between the threshold voltage (V_T) and some desired value (corresponding to a particular inversion-layer density) at a frequency of $\lesssim 1000$ Hz. The detector signal coherent with this square-wave modulation was lock-in-amplified and the dc output (proportional to the difference between the transmitted light signal with some desired inversion-layer electron density and that with an inversion-layer density of zero) was converted to a digital signal by a 12-bit analog-to-digital converter. After signal-averaging a number of scans, the Fourier-transformed difference spectrum was ratioed to a background spectrum obtained with $V_G = V_T$ and chopped light. The inverted ratio provides a "differential absorption spectrum" directly for these very weak absorption lines (percent absorption versus wave numbers).

IV. EXPERIMENTAL RESULTS

A. (110) surface

Some experimental data for the (110) surface are shown in Figs. 2 and 3 for the infrared electric field polarized parallel and perpendicular to the surface, respectively (from samples 1 and 3, respectively). It has been verified in separate measurements on chips from these same wafers that the valley degeneracy g_v is equal to 4 for these samples.[25] In both sets of data, approximately the full equilibrium depletion charge was established; this can be seen from the line shapes, where the 0-2 transition is well separated and clearly resolved from the 0-1 transition. These data are summarized in Fig. 4 and the calculations of Ando are shown for comparison. Ando's calculations are for twofold-degenerate samples; there will be a small shift (~ 1–2 meV) to lower energies for the fourfold-degenerate case due to the smaller Fermi energy for a given n_s and the resulting smaller exchange lowering of the ground subband relative to the excited subbands. The data exhibit a substantial shift to lower energies for the $E_{||}$ surface polarization, compared with the $E_\perp$ surface polarization, of approximately 30–35 %. The magnitude of this difference is approximately constant within the scatter over the range of n_s investigated. An indication of the variation in transition energy from one sample to another (from the same wafer) is provided by comparing the square and triangular data points. This shift is roughly 1–2 meV (due to variations in depletion charge) compared with a 6-meV difference between $E_\perp$ and $E_{||}$ data. The depletion charge for these samples could not be directly determined experimentally, but from the magnitude of the energy difference between the 0-1 and 0-2 transitions, it is estimated to be $\lesssim 10^{11}$ cm^{-2}, consistent with the substrate doping.

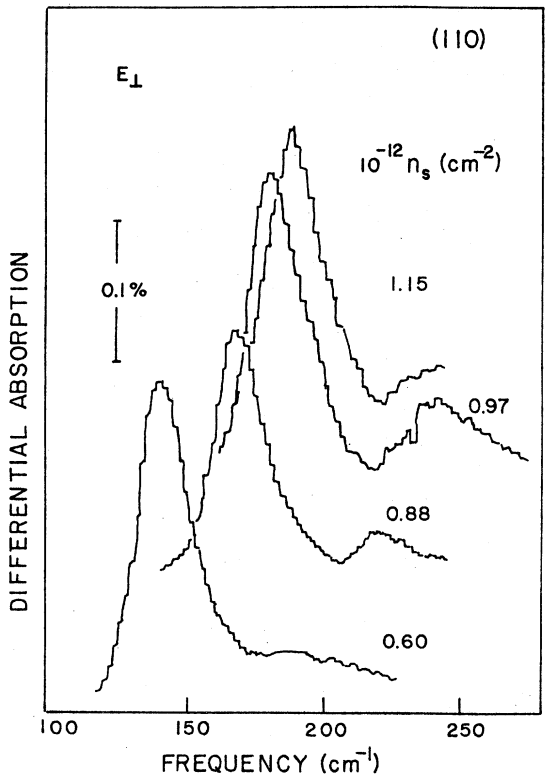

FIG. 2. Differential absorption spectra at 4.2 K for a (110) sample (sample 1) with the ir electric field polarized perpendicular to the surface (parallel to [110]). Nearly equilibrium depletion charge was established in this sample. Electron densities are indicated.

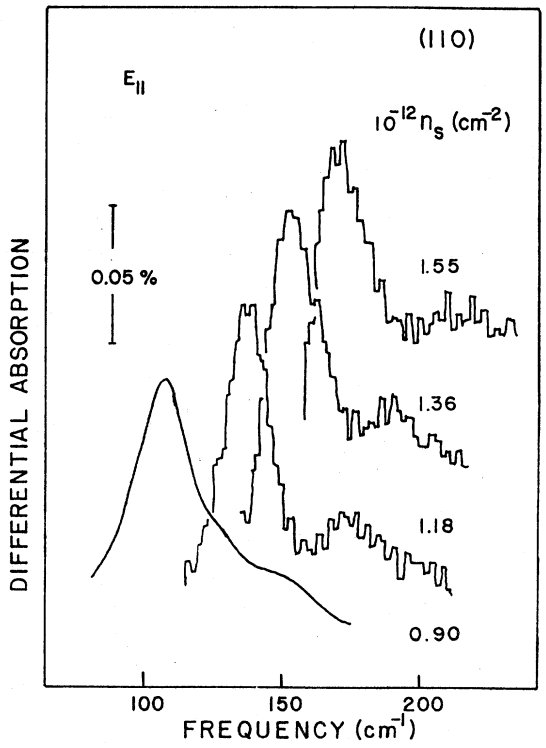

FIG. 3. Differential absorption spectra at 4.2 K for a (110) sample (sample 3) with the ir electric field polarized parallel to the surface. The "noise" on the three highest-density spectra is a result of multiple internal reflection interference. This has been smoothed on the lowest-density curve. This sample had nearly equilibrium depletion charge established. Electron densities are indicated.

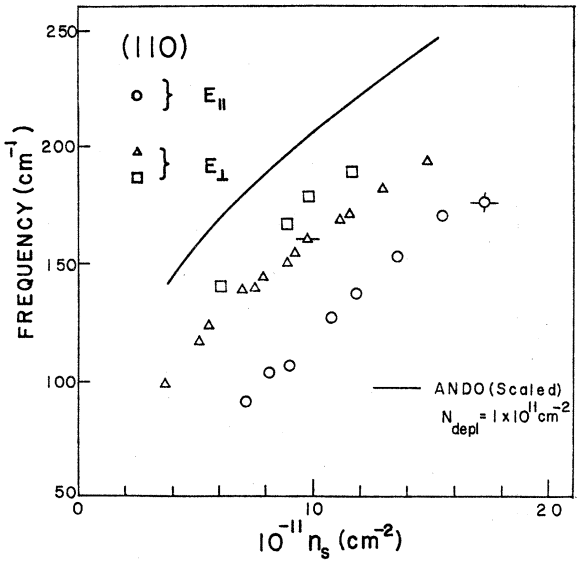

FIG. 4. Summary of data for Si(11) (samples 1 and 3) for the 0-1 transition for the electric-field polarized parallel and perpendicular to the surface. ○—sample 3, chip 3. △—sample 1. □—chip of sample 1 with slightly higher depletion charge. The solid line is taken from Ref. 20 and scaled to the indicated depletion charge. Typical error bars are indicated.

Additional data are shown in Figs. 5 and 6 for quasiaccumulation samples (chips from samples 2 and 3). These samples exhibited quasiaccumulation behavior at 4.2 K due to rectifying substrate contacts that provided a forward substrate bias at low temperature. The depletion charge is not well known, but from the line shapes (crowding together of the 0-2 and higher transitions), it is estimated to be in the low, 10^{10}-cm^{-2} regime. These data

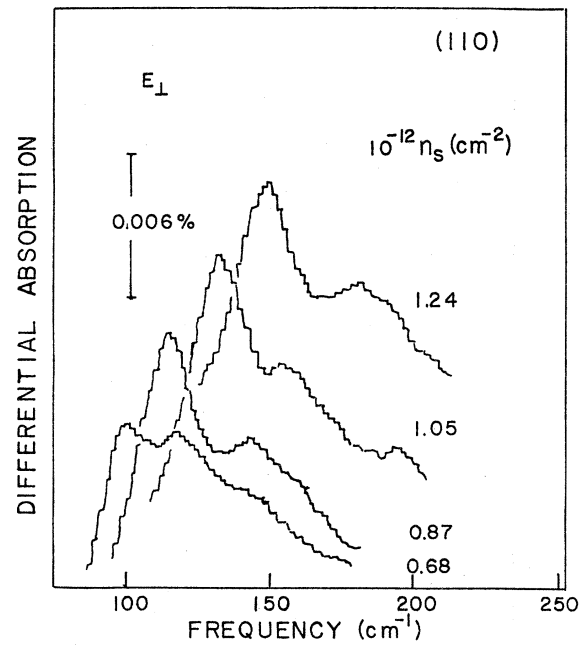

FIG. 5. Differential absorption spectra at 4.2 K for a (110) sample (sample 2) with the ir electric field polarized perpendicular to the surface. This sample had a low depletion charge ($\sim 10^{10}$ cm^{-2}). Electron densities are indicated.

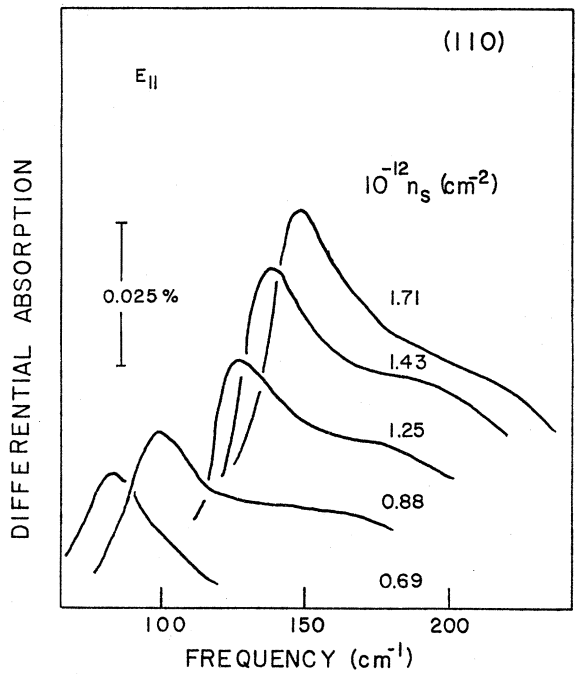

FIG. 6. Differential absorption spectra for sample 3, chip 4 at 4.2 K with the ir electric field polarized parallel to the interface. This sample had a low depletion charge ($\sim 10^{10}$ cm^{-2}). Multiple internal reflection interference oscillations have been smoothed in these data. Electron densities are indicated.

and additional data for the 0-1 transition are summarized in Fig. 7, together with a calculation[21] for twofold valley degeneracy and accumulation conditions. Again, an indication of the scatter in the transition energies for several different samples taken over a period of several months is provided by this figure. The scatter is typically less than 1 meV for $E_{||}$ or $E_{\perp}$, while the separation between $E_{||}$ and $E_{\perp}$ is 3—4 meV out of $\sim$12—20 meV (20—25%). The

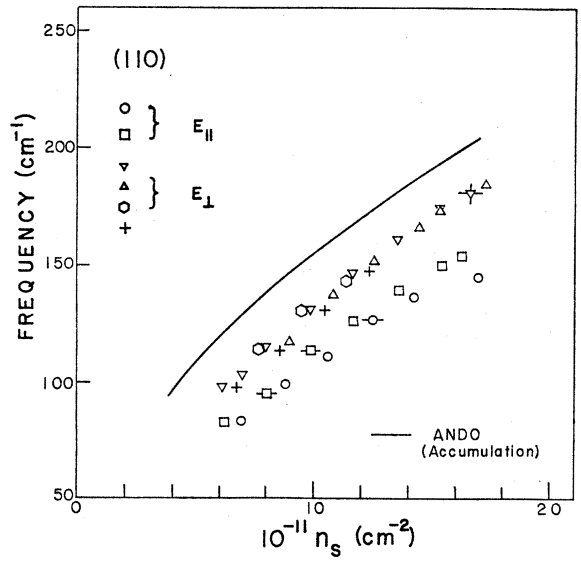

FIG. 7. Summary of transition-energy data for the 0-1 transition for samples 2 and 3. □ and ○—sample 3, chip 4; ▽, △, **O**, and +—two chips of sample 2. The solid line is taken from Ref. 20. Typical error bars are indicated.

magnitude of the difference increases with increasing electron density.

B. (111) surface

Some experimental data for a Si(111) sample (sample 4) having twofold valley degeneracy ($g_v=2$) is shown in Fig. 8. The valley degeneracy was determined from magnetoconductance oscillations on Hall bars taken from adjacent chips. The data are dominated by one strong line with much weaker lines at both higher and lower energies, the latter is only clearly observed between $n_s=4\times10^{11}$ and 1.3×10^{12} cm^{-2}.

A polarization study at two different electron densities is shown in Fig. 9. The solid curves are taken with light polarized normal to the interface. The dotted curves show the spectra for the same sample with a linear polarizer placed in front of the prism to admit only light polarized parallel to the interface ($E_{||}[1\bar{1}0]$). Except for a small shift (less than 1 meV) to higher energies and a reduction in intensity for the $E_{||}$ ($E_{||}[1\bar{1}0]$) data, the curves are very similar.

These data and other data for the dominant peak and the weak, low-energy peak are summarized in Fig. 10, which also includes calculated transition energies and subband separations (for the ground and first excited subbands) for twofold-degenerate samples from Ref. 4. These data are from two chips of sample 4 taken in several runs over a period of several months. As can be seen, there is some scatter in the data (of the order of 1.5 meV) due to small changes in depletion charge. Within the scatter shown in Fig. 10, it is not possible to conclude that there *is* a shift. Although the data of Fig. 9 appear to show a slight shift to higher frequency for $E_{||}$, it appears that this is due to a slightly higher depletion charge.

The energy position of the weak, low-energy peak increases with increasing n_s somewhat more slowly than that of the dominant peak. Between 4×10^{11} and 1.3×10^{12} cm^{-2} the *separation* between these peaks increases by approximately 30%. Substrate-bias studies show that these two peaks shift exactly in concert with depletion charge at constant n_s. (Their separation is constant at 40 cm^{-1} to within ±1 cm^{-1} for depletion charge between 1×10^{11} and 4×10^{11} cm^{-2}.) The implication of these results regarding the identification of the various peaks is discussed in the next section.

Several samples that underwent special Ar-annealing treatments and exhibited sixfold valley degeneracy were also investigated. These samples were consistently of poorer quality than the "normal" (twofold) samples discussed above (see Table I). All of these samples had substantial negative threshold voltages (indicative of relatively large amounts of net positive oxide charge) and much poorer peak effective mobilities (typically 1000 cm^2/V sec or less).

An example of data from this group of samples (samples 5 and 6 of Table I) is shown in Fig. 11. The upper panel shows data for $E_\perp$ and the lower panel shows data for $E_{||}$. The lines are quite broad in each case. Apparently due to problems with establishing an equilibrium de-

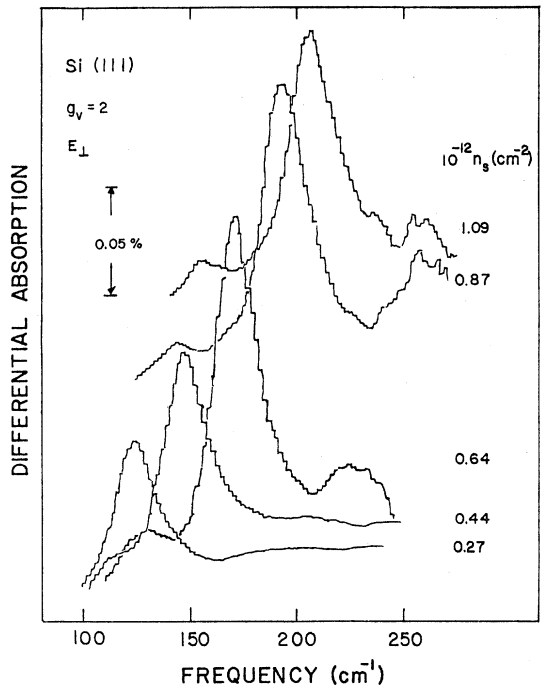

FIG. 8. Differential absorption spectra for a (111) sample (sample 4, chip 1) at 4.2 K with the ir electric field polarized perpendicular to the interface. Depletion charge is 10^{11} cm^{-2} for this sample. Electron densities are indicated.

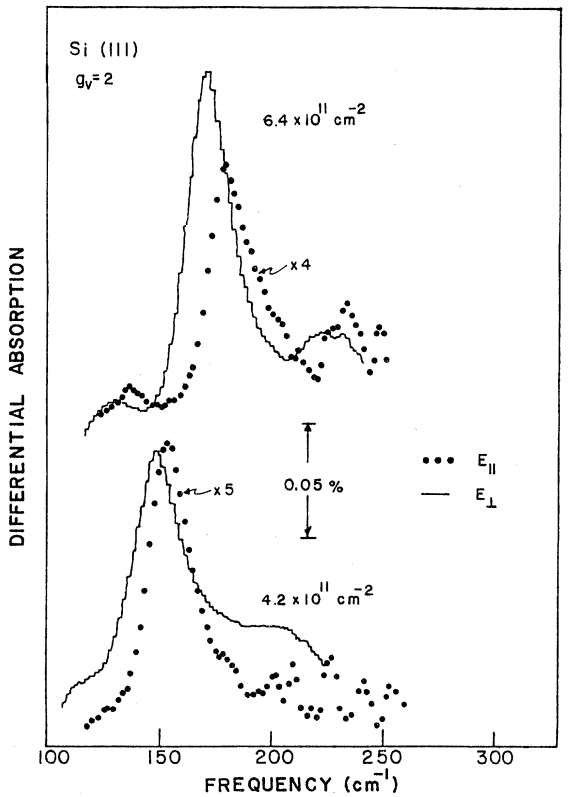

FIG. 9. Differential absorption spectra for a Si(111) MOSFET (sample 4, chip 1) with valley degeneracy $g_v=2$ for the ir electric field polarized parallel (solid line) and perpendicular (solid circles) to the surface. There is a very slight shift to higher energies for the $E_{||}$ data, but it appears that these data are also for a slightly higher depletion charge. Electron densities at which the data were taken are indicated.

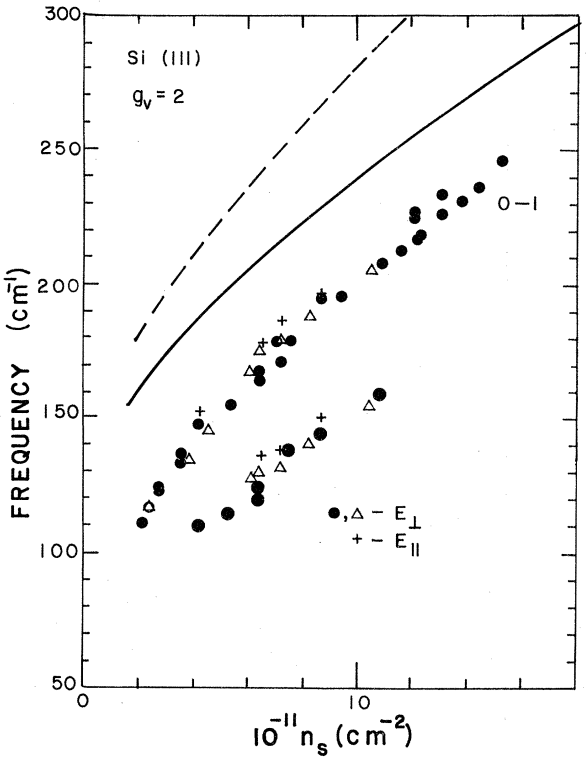

FIG. 10. Comparison of experimental data for the 0-1 transition taken from two Si(111) samples with theoretical calculations for the subband separation (solid line) and the transition energy (dashed line). The theoretical results are from Ref. 4. ● and +—sample 4, chip 1; △—sample 4, chip 2. The higher-energy data points are for the 0-1 transition. The lower-energy data points are discussed in the text.

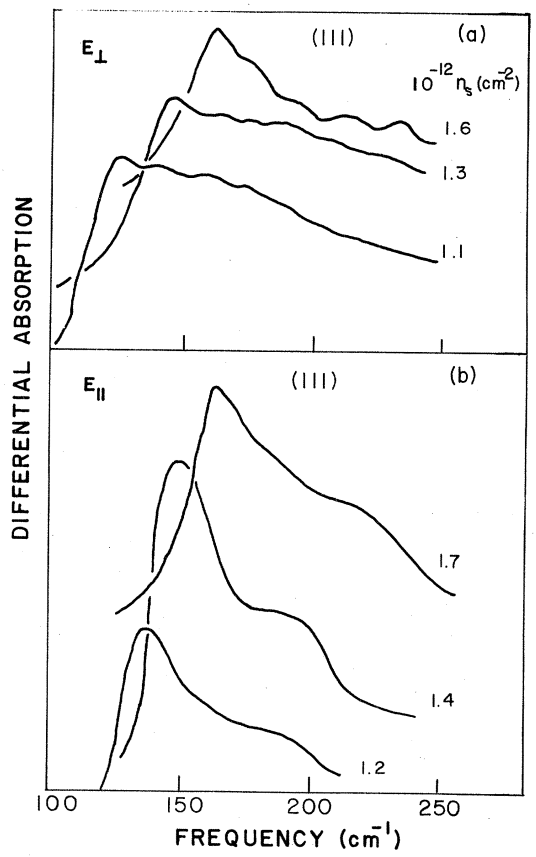

FIG. 11. (a) Differential absorption spectra for a (111) sample (sample 5, chip 2) at 4.2 K with the ir electric field polarized perpendicular to the surface. These lines have a characteristic "accumulation" line shape. (b) A (111) sample (sample 6, chip 3) at 4.2 K with the ir electric field polarized parallel to the interface. The lines, although broad, have a shape more characteristic of substantial depletion charge. Electron densities are indicated.

pletion charge, the $E_\perp$ data exhibit a quasiaccumulation line shape in which the 0-2 and higher transitions merge together as a broad "shoulder" on the high-energy side of the main peak. On the other hand, the data for $E_{||}$ (semitransparent Cr gates) show a reasonably well-resolved and separated 0-2 transition. A compilation of these data for the 0-1 transition along with data from another chip from sample 6 is shown in Fig. 12. In the latter case, data obtained at two different values of substrate bias, -2 and -5 V, as well as data for zero substrate bias, are presented. Some of the data for the dominant peak from sample 4 of Fig. 10 are also plotted for reference. All of the 0-1 data for the Ar-annealed samples at zero substrate bias are 8—10 meV below the data for the "normally processed" sample. Data for the two different chips from sample 6 at zero substrate bias (with $E_{||}$) exhibit little scatter (good reproducibility). Above $n_s = 1.2 \times 10^{12}$ cm^{-2} these data are systematically very slightly lower than the data for sample 5 ($E_\perp$) from the same processing run. However, since sample 5 exhibits quasiaccumulation line shapes, these data should be shifted to higher energies to account for differences in depletion charge and to compare them with the data of sample 6. Analysis of the substrate-bias data from second chip of sample 6 (inverted triangles and open triangles) is consistent with the presence of substantial depletion charge in these samples ($\sim 1 \times 10^{11}$ cm^{-2}) at zero substrate bias. Assuming that the depletion charge in sample 5 is very small, these data would then have to be scaled to higher energies by approximately 4—6 meV (30—50 cm^{-1}) over the range of electron densities shown to compare with sample 6. This would make the data for $E_\perp$ fall roughly 30% higher than the $E_{||}$ data. However, this procedure is qualitative at best and filled with uncertainties. For example, the depletion-charge dependence of the transition energy obtained from the substrate-bias data for sample 6 agrees best with either the triangular potential model or with Ando's calculations for (100) if it is assumed that the actual electron density is substantially less than indicated. The plotted electron density is obtained from the V_G, the liquid-nitrogen temperature V_T, and the oxide thickness. A reduction in actual n_s at 4.2 K could take place if there were a large density of inactive trap states at the oxide-Si interface resulting from the Ar-annealing step. Owing to the very poor mobility of these samples, Shubnikov—de Haas oscillations were observable in Hall bars from these samples only in the second derivative at the highest fields available. Thus, the threshold voltage could not be determined by extrapolation with any degree of confidence, and as a result, it was not possible to verify this hypothesis by comparison with the 77-K

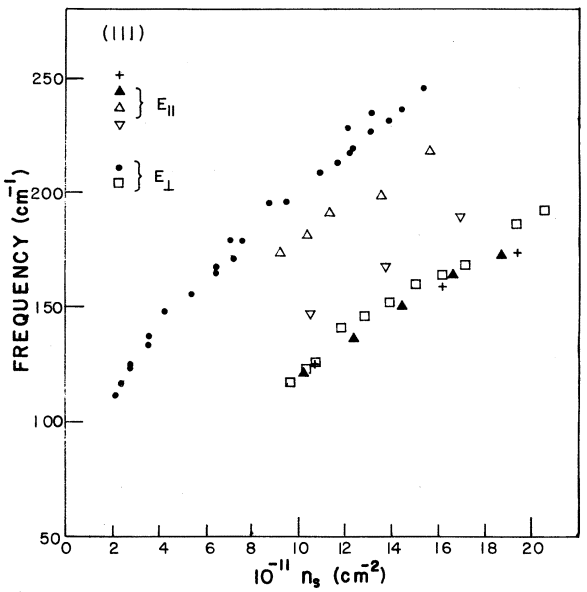

FIG. 12. Summary of transition-energy data for the 0-1 transition for several (111) samples at 4.2 K. ●—sample 4, chip 1; triangles—sample 6, chip 5; ▲—$V_{sub}=0$; ▽—$V_{sub}=-2$ V; △—$V_{sub}=-5$ V); +—sample 6, chip 4; □—sample 5. The data from sample 4, chip 1 are plotted for comparison purposes. This sample had $g_v=2$.

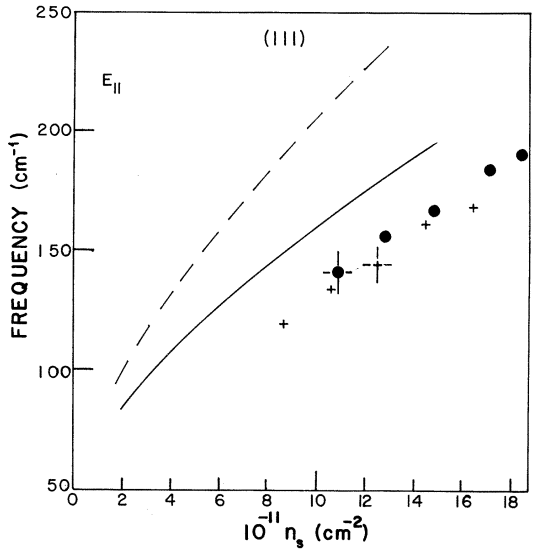

FIG. 13. Transition-energy data for the 0-1 transition at 4.2 K for two (111) samples with the ir electric field polarized parallel to the surface. ○—sample 7; +—sample 8. The results of Ref. 4 for $g_v=6$ are shown for comparison. In order to obtain the results shown for $N_{depl}=1.5\times10^{10}$ cm^{-2}, an approximate adjustment in the results of Ref. 4 (for $N_{depl}=1\times10^{11}$ cm^{-2}) was made by *subtracting* off the difference in depletion charge contribution in the triangular potential approximation. Solid line denotes the transition energy. Dashed line denotes the subband separation. Typical error bars are indicated.

threshold voltage. A reduction in n_s of $3-5\times10^{11}$ cm^{-2} for samples 5 and 6 would bring these data into reasonable agreement with the data of sample 4. Another possible explanation for the large shift is a substantial reduction in exchange correlation effects due to the large "impurity" scattering in the sixfold-degenerate samples.[12]

Data from the final set of (111) samples (samples 7 and 8) are shown in Fig. 13. These samples were fabricated on 1000-Ω cm *p*-type Si, and the corresponding calculated equilibrium depletion charge is $\sim1.5\times10^{10}$ cm^{-2}. Thus, these samples should be much less susceptible to problems associated with establishing an equilibrium depletion charge, since the difference in transition energy between zero depletion charge and 1.5×10^{10} cm^{-2} is only about -2 meV (within the experimental scatter). Devices were fabricated *only* with thin-Cr-gate metallizations, sample 7 was fabricated with Ar annealing of the gate oxide, and sample 8 was fabricated with "normal" N_2 annealing. The valley degeneracy was not experimentally determined for these samples.

Owing to the inferior sample quality, the spectra were broad and rather poor, leading to relatively large uncertainties in peak positions (typically $\pm$ 5 cm^{-1}). Within this experimental uncertainty, there is no clear difference between the 0-1 transition energies for the N_2-annealed (presumably twofold) and Ar-annealed (presumably sixfold) samples. It should be noted that at a given value of n_s, these data are consistently about 2 meV higher in energy than the $E_{||}$ data of sample 6 at zero substrate bias. If sample 6 has a depletion charge of $\sim1\times10^{11}$ cm^{-2} as asserted above, then the 0-1 transition energies should be *higher* than the equivalent data for sample 7 by several meV. Again, this discrepancy could be a result of differences in the actual values of n_s due to a large density of trap states at the oxide-Si interface, the magnitude of which depends on the sample processing.

V. DISCUSSION

In this section the experimental results described previously are compared with the detailed results for the polarization dependences obtained by Yi and Quinn,[4] and the relevance of these results to the various models that attempt to explain the anomalous valley degeneracy on the (111) surface is considered. The models to be considered include strain, strain-enhanced exchange-correlation effects, and CDW's. The results of strain and strain-enhanced many-body effects should be essentially the same as regards the optical measurements, and these will be considered as a single possibility. Particular results which must be reconciled with predictions based on the models are the polarization dependences of the transition energies for both surfaces, the low-frequency transitions seen in the twofold-degenerate (111) samples, and the large differences in the intersubband transition energies for (111) samples that have undergone different annealing treatment during processing.

A. (110) surface

The results of Yi and Quinn[4] for the (110) surface are summarized in Table II. These results were obtained through the application of linear-response theory to a quasi-2D system assuming an ideal abrupt interface, and the use of a two-level system to simplify the treatment of the depolarization and final-state—interaction corrections.

In general, for an arbitrary surface orientation, the off-diagonal elements of the anisotropic effective-mass tensor

TABLE II. Polarization selection rules and transition frequencies for the 0-1 transition for the Si(110) surface (after Ref. 4). The quantities α and β are described in the text.

Polarization \ Valley degeneracy	Fourfold	Twofold
[110]	$\omega_{res}=\omega_{10}(1+\alpha_{11}-\beta_{11})^{1/2}$	$\omega_{res}=\omega_{10}(1+\alpha_{11}-\beta_{11})^{1/2}$
[1$\bar{1}$0]	$\omega_{res}=\omega_{10}(1-\beta_{11})^{1/2}$	$\omega_{res}=\omega_{10}(1+\alpha_{11}-\beta_{11})^{1/2}$
[001]	No resonance	No resonance

of the Si conduction band couple the motion of electrons parallel and perpendicular to the surface. The physical reason for this can be seen qualitatively following the treatment of Ref. 24. The Hamiltonian for an electron in valley v in the usual coordinate system [Fig. 1(a)] can be written as

$$H^{(v)}=\tfrac{1}{2}\sum_{i,j=x,y,z} w_{ij}^{(v)}p_i p_j+V(z)\ , \tag{4}$$

where $w_{ij}^{(v)}$ is the inverse effective-mass tensor for valley v, p_i is the momentum operator, and $V(z)$ is the potential energy. For example, for the z-oriented valleys of Fig. 1(a),

$$w_{ij}=\begin{bmatrix} m_t^{-1} & 0 & 0 \\ 0 & m_t^{-1} & 0 \\ 0 & 0 & m_l^{-1} \end{bmatrix}\ . \tag{5}$$

In the new coordinate system appropriate to the particular surface of interest, the Hamiltonian is transformed by a unitary (rotation) transformation to

$$\tilde{H}^{(v)}=\tfrac{1}{2}\sum_{\mu,\nu=x,y,z} w_{\mu\nu}^{(v)}p_\mu p_\nu+\tfrac{1}{2}w_{zz}^{(v)}p_z^2+V(z)\ , \tag{6}$$

with

$$\tilde{w}_{\mu\nu}^{(v)}=w_{\mu\nu}^{(v)}-w_{\mu z}^{(v)}w_{\nu z}^{(v)}/w_{zz}^{(v)}\ .$$

The corresponding velocity operators are given by

$$\tilde{v}_\nu^{(v)}=\sum_{\nu=x,y}\tilde{w}_{\mu\nu}^{(v)}p_\nu+w_{\mu z}^{(v)}p_z\ . \tag{7}$$

Since electric dipole transitions are proportional to matrix elements of the velocity operator, Eq. (7) determines the polarization selection rules. In general, for non-{001} surfaces, the second term of Eq. (7) will allow intersubband contributions (the operator p_z couples the subband states) even when the incident infrared electric field is polarized in the surface plane (x-y plane). This will be the case except for specially symmetric circumstances, where $\alpha_{\mu z}=0$, for example, $\vec{E}||[001]$ in Table II.

The depolarization effect depends on the total current induced perpendicular to the particular surface ($j_{ind}=\sum_{(v)}ne\tilde{v}_\mu^{(v)}$). Thus, even when currents exist in the z direction for individual ellipsoids (i.e., $\alpha_{\mu z}\neq 0$), whenever there is a fully symmetric ground state [such as $g_v=4$ for (110) or 6 for (111)], the *total* induced current will vanish, and there is no depolarization shift. This is the case for [1$\bar{1}$0] polarization and fourfold degeneracy in Table II ($\alpha_{11}=0$). The individual currents for ellipsoids x, $\bar{x}$, y, and $\bar{y}$ add up to zero. For reduced symmetry, this cancellation does not take place and the depolarization shift is present.

The question of the vertex corrections (final-state interactions) is more complex. Ando *et al.*[24] claim that a similar cancellation to that occuring for the depolarization shift takes place, and most of the vertex corrections cancel out for the completely symmetric ground state. On the other hand, as can be seen from Tables II and III, the results of Yi and Quinn[4] for a two-level system include the complete vertex correction for an $E_{||}$ excitation even when the depolarization shift cancels out for the symmetric ground state. Thus, the simple-minded use of the formulas of Tables II and III to analyze experimental data should be viewed with some caution. In addition, it should be emphasized that these results were obtained for

TABLE III. Polarization selection rules and transition frequencies for the 0-1 transition for the Si(111) surface (after Ref. 4). The quantities α and β are described in the text.

Polarization \ Valley degeneracy	Sixfold	Twofold	
		[11$\bar{2}$]-oriented valleys	Pairs of valleys tilted with respect to [1$\bar{1}$0] or [11$\bar{2}$]
[111]	$\omega_{res}=\omega_{10}(1+\alpha_{11}-\beta_{11})^{1/2}$	$\omega_{res}=\omega_{10}(1+\alpha_{11}-\beta_{11})^{1/2}$	$\omega_{res}=\omega_{10}(1+\alpha_{11}-\beta_{11})^{1/2}$
[1$\bar{1}$0]	$\omega_{res}=\omega_{10}(1-\beta_{11})^{1/2}$	No resonance	$\omega_{res}=\omega_{10}(1+\alpha_{11}-\beta_{11})^{1/2}$
[11$\bar{2}$]	$\omega_{res}=\omega_{10}(1-\beta_{11})^{1/2}$	$\omega_{res}=\omega_{10}(1+\alpha_{11}-\beta_{11})^{1/2}$	$\omega_{res}=\omega_{10}(1+\alpha_{11}-\beta_{11})^{1/2}$

a two-level model, and interactions among subband oscillators, which take place when the vertex and depolarization effects do not completely cancel, have been neglected. Such interactions lead to an exchange of relative intensities and shifts in peak positions,[2,4,20] which can be quite large for samples with low depletion charge. This further complicates data analysis.

With this background and these caveats in mind, we now consider the (110) data. The data summarized in Figs. 4 and 7 exhibit substantial shifts to higher energies for $E_\perp$ compared with $E_{||}$. From Table II this is consistent only with fourfold degeneracy. Thus these data are in agreement with the Shubnikov–de Haas results. Recent subband measurements of Nee *et al.*[26] are in qualitative agreement with these data where they overlap. These authors have also carried out polarization-rotation studies in the (110) plane and have verified the polarization selection rules of Table II for fourfold degeneracy.

The 0-1 transition energies for both very small depletion charge and a depletion charge less than approximately 10^{11} cm^{-2} are consistently lower than the calculations of Ando shown in Figs. 7 and 4. However, given the approximate nature of the calculations and the experimental uncertainty in depletion charge, the significance of these differences is not clear.

Before turning to the (111) data, one final result should be mentioned. For the $E_{||}$ sample (sample 3) of Fig. 7, an additional line was observed at lower frequencies than 0-1. Over the range $n_s = 1\times10^{12}$–1.75×10^{12} cm^{-2} this line moved from 80 to 85 cm^{-1}, increased in intensity, and broadened from $\sim$2 meV full width at half maximum (FWHM) to $\sim$4 meV FWHM. It was not observed in another chip of sample 3 in which a nearly equilibrium depletion charge was established ($E_{||}$ data of Fig. 4). The origin of this line is not known at this time.

B. (111) surface

The results of Yi and Quinn[4] for the polarization selection rules and transition frequencies for the (111) surface are given in Table III. For the twofold-degenerate situation, there are two distinct possibilities to be considered: (1) The lowest set of valleys is that pair oriented along the $[11\bar{2}]$ direction [see Figs. 1(a) and 1(c)], and (2) the lowest set of valleys is a pair tilted with respect to the $[1\bar{1}0]$ or $[11\bar{2}]$ directions. In case (1), for reasons analogous to those discussed for the (110) surface, there is *no* subband resonance for the infrared electric field in the plane of the surface polarized along $[1\bar{1}0]$ ($w_{\mu z}^{(v)}=0$ in this case; x is taken along the $[1\bar{1}0]$ direction and y is taken along the $[11\bar{2}]$ direction). For the $\vec{E}||[11\bar{2}]$ direction, since this is a situation of reduced symmetry, the depolarization shift is present. In case (2), the lowest valleys always have an off-diagonal component w_{xz} or w_{yz}, so that subband transitions are allowed for both polarizations with the depolarization shift present.

The sixfold-degenerate situation, possessing full symmetry, is analogous to the fourfold-degenerate situation for (110). However, in this case, there is no polarization in the plane for which the off-diagonal component $w_{\mu z}$ vanishes. Hence, subband transitions with *no depolarization shift* are permitted for both $\vec{E}||[1\bar{1}0]$ and $\vec{E}||[11\bar{2}]$.

For the (111) surface, Yi and Quinn[4] have carried out numerical calculations of the absorption lines for a three-level system with $g_v=2$, including depolarization and vertex corrections. There are substantial differences in the calculated values of these quantities for a depletion charge of 10^{11} cm^{-2} and an electron density of 10^{12} cm^{-2}. Yi and Quinn find a large transfer of oscillator strength from 0-1 to 0-2, making 0-2 the dominant feature in the calculated spectrum for equal linewidths. This effect must be considered in the discussion of the experimental observations for $g_v=2$.

This situation has been considered as a possible explanation of the low-frequency line of Figs. 8–10, namely that the weak, low-frequency feature is actually 0-1, while the dominant peak is 0-2. This explanation has been rejected on the basis of the substrate-bias studies. *No* relative shift was found between these two features over a factor of 4 in depletion charge, and the relative intensities remained constant. This behavior is not consistent with the above explanation since the coupling depends on the individual transition frequencies which are, in turn, a strong function of depletion charge. Hence, it is concluded that the dominant feature is, indeed, the 0-1 transition, and it is necessary to look elsewhere for an explanation of the low-frequency line. In addition, this identification implies that the calculated depolarization shift and vertex corrections are possibly incorrect (at least the difference is incorrect), and they are actually nearly equal.

Two other possible explanations of the low-frequency peak have been considered. One possibility arises if the removal of the valley degeneracy is attributed to a CDW ground state. In this case, the low-energy feature could be due to a bonding-to-nonbonding or -antibonding transition. This is consistent with the appearance of the low-energy feature only for twofold valley degeneracy, and requires that the valley splitting be less than the subband separation (10–25 meV, consistent with the estimates made by Tsui and Kaminsky[6]). The CDW ground state also allows the possibility of a transition from the ground subband of the bonding state to the excited subband of the antibonding state, which should be higher in energy than the subband transition between bonding levels, and should occur only for light polarized parallel to the interface.[16] There is no evidence of such a transition in the data. In any case, it appears that the CDW can be ruled out on the basis of the considerations discussed in Sec. II.

A second possibility is that this structure results from a transition between the ground-state level of the lowest valley and that of one of the higher valleys, a normally forbidden intervalley transition (due to crystal momentum conservation). Large surface roughness on a spatial scale with Fourier components corresponding to the necessary q vectors could admix band-edge wave functions of the two sets of valleys and relax the momentum conservation. In this case, the transition energy measures the valley splitting directly (13–20 meV between $n_s=4\times10^{11}$ and 1.1×10^{12} cm^{-2}, again consistent with Ref. 6). The n_s and depletion-charge dependences for such a transition have not been calculated, but from results on the (100) surface, similar dependences for the 0-1 and ground-

state—to—ground-state energies might be expected.

The polarization dependence of the spectra are in agreement with the results summarized in Table III for twofold degeneracy with a pair of valleys lowest in energy whose principle axes are tilted with respect to the $[1\bar{1}0]$ or $[11\bar{2}]$ axes of the crystal. Hence, the transport measurements and optical measurements for these samples are internally consistent.

On the other hand, the experimentally determined 0-1 transition energies for these samples are 9—10 meV below the *transition energies* calculated by Yi and Quinn (Fig. 10). The agreement is substantially better with the calculated *subband energy separations* (equal to the transition energy if the depolarization and vertex corrections cancel). This may be considered further evidence for nearly equal depolarization and vertex corrections. These remaining differences could be partially accounted for by slight overestimates of the calculated energy separation due to the variational approach used in Ref. 4 and an experimental depletion charge slightly less than 1×10^{11} cm^{-2}.

For the Ar-annealed (sixfold) samples of Fig. 12, the 0-1 transition energies are 9—10 meV below those for the twofold samples discussed above. The shift is in the direction expected from the difference in exchange-correlation effects between the two cases but is *much larger* in magnitude than calculated.[11] The shift is also in the direction expected between twofold and sixfold samples for $E_{||}$ (see Table III), but again, it is considerably larger than would be expected on this basis alone. Yi and Quinn[19,27] have recently calculated the transition energies for (111) inversion layers for both twofold and sixfold degeneracies including inhomogeneous stress and many-body effects. Shifts of this size can be obtained by appropriate choices of stress parameters. However, the observed transition energies in both cases are much smaller than their calculations predict. The observed energies for the sixfold samples are actually below their calculated Hartree energies.

These large discrepancies are difficult to explain, as is the apparently *very* small shift between $E_\perp$ and $E_{||}$ spectra in the raw data of Fig. 12. It appears that the former discrepancy could be related to degradation of the interface of the Ar-annealed samples as discussed in Sec. IV. Certainly, part of this degradation is due to increased positive oxide charge which would cause shifts to higher energies for $E_\perp$ transitions.[28] However, as discussed in the preceding section, there are also trapping centers and potential fluctuations that could trap carriers in optically inactive states at low temperature. This would *reduce* the effective n_s below that determined from the capacitance relationship (and plotted in Fig. 12), and would improve the agreement considerably.

The discrepancy between the substantial shifts between spectra obtained with $E_{||}$ and $E_\perp$ predicted in Table III and the experimental results of Fig. 12 is clearly related to the absence of substantial depletion charge in the $E_\perp$ samples. The experiment and theory are reconciled by the assertions and discussion in Sec. IV B. However, due to these large uncertainties, it can only be stated that it is *likely* that the $E_\perp$ data for sixfold degenerate samples are shifted by several meV to higher energy than the $E_\perp$ data. This cannot be a firm conclusion from the present work.[29–31]

Finally, the $E_{||}$ transition energies of Fig. 13 for Ar- and N_2-annealed samples can also be reconciled with the remaining data by the above arguments concerning large densities of inactive trap states in samples 5 and 6. However, the lack of any observable difference between N_2- and Ar-annealed samples within experimental scatter is not consistent with the calculations which predict a shift to higher energies for the twofold samples, since the depolarization shift is present. A firm conclusion regarding this observation is not possible at this time since the valley degeneracy could not be determined for these samples due to the very poor mobility. Again, as can be seen in Fig. 13, these data lie below the calculation for both the subband separation and the transition energy, but much closer to the former.

There are implications of this work regarding the underlying mechanism for the anomalous valley degeneracy on (111) surfaces, in spite of the experimental uncertainties. The present results are generally consistent with the calculations of Yi and Quinn[4] for both (110) and (111) (with less certainty) and given the other arguments against the CDW model, some variation of the stress model[6,27] is preferred. However, there are still some perplexing problems remaining. The magnitude of the experimental transition energies is consistently smaller than that calculated for both the (110), and especially the (111) surfaces, even with posssible ameliorating effects taken into account. Additional weak, low-energy structure for the twofold (111) samples is not adequately explained, and the importance of many-body effects in determining the valley degeneracy has not been unambiguously determined.

VI. SUMMARY AND CONCLUSIONS

Frequency-domain intersubband spectroscopy has been carried out on (110) and (111) Si n-type inversion layers. Polarization-dependence studies on the (110) samples with measured fourfold valley degeneracy are in good agreement with recent calculations of Yi and Quinn.[4] Measured transition energies are consistently lower by several meV than those calculated. Both normally processed (111) samples and (111) samples which underwent special Ar-annealing treatment were studied. Normally processed samples were twofold degenerate as determined from Shubnikov—de Haas measurements and polarization-dependence studies, again all in good agreement with Ref. 4. However, measured transition energies are much lower than those calculated.[4] Better agreement is obtained with the calculated subband separations, and this observation combined with the observed relative intensities implies that the depolarization and vertex corrections nearly cancel, in disagreement with calculations. Transition energies for the Ar-annealed samples for both $E_{||}$ and $E_\perp$ are 9—10 meV below those for the normally processed samples having nominally the same depletion charge. A portion of this disparity is apparently due to very small depletion charge in the $E_\perp$ samples. With this taken into account, the polarization dependence for the sixfold samples is consistent with the results of Ref. 4. The remaining disparity

in transition energy between Ar-annealed and N_2-annealed samples may be due to interface degradation in the Ar-annealed samples, resulting in a large density of optically inactive trap states at low temperature. The results of these studies are consistent with large-stress results or results from studies of samples stress enhanced by many-body effects as the underlying mechanism for the anomalous valley degeneracy.

(Note added.) After this manuscript was submitted, the authors were made aware of results of Martelli, Mazuré, and Koch (unpublished), in which a small, but apparently real, shift has been observed for $E_{||}$ and $E_{\perp}$ on Si(111) n-type accumulation layers having undergone "normal" processing (presumably twofold degenerate). This small shift would not be outside systematic error in the present work on inversion layers due to small variations in depletion charge from run to run. It is not consistent with the results of Ref. 4 for twofold-degenerate samples and is much smaller than would be expected from sixfold-degenerate samples due to the presence of the depolarization shift in the perpendicular polarization and not in the parallel polarization.

ACKNOWLEDGMENTS

The authors are grateful to J. J. Quinn and K. S. Yi for many helpful discussions and for making available the results of their work prior to publication. Thanks are also due to the Naval Research Laboratory Microelectronics Processing Facility, and Mr. P. Reid and Dr. M. Peckerar in particular, for the processing of the devices used in this study. The authors are also grateful to F. Koch for sharing results prior to publication and discussions, and to J. Kotthaus for discussions of work prior to publication. One of us (T. C.) acknowledges support of a Naval Research Laboratory—National Research Council Resident Research Associateship at the Naval Research Laboratory. The work of another of us (B. D. M.) was supported in part by the U. S. Office of Naval Research.

*Present address.

[1]See, e.g., the recent review by T. Ando, A. B. Fowler, and F. Stern, Rev. Mod. Phys. 54, 437 (1982).

[2]B. D. McCombe, R. T. Holm, and D. E. Schafer, Solid State Commun. 32, 603 (1979).

[3]See, e.g., T. Ando, Phys. Rev. B 13, 3466 (1976).

[4]K. S. Yi and J. J. Quinn, Phys. Rev. B 27, 2396 (1983).

[5]A. A. Lakhani and P. J. Stiles, Phys. Lett. 51A, 117 (1975); T. Neugebauer, K. von Klitzing, G. Landwehr, and G. Dorda, Solid State Commun. 17, 295 (1975).

[6]D. C. Tsui and G. Kaminsky, Phys. Rev. Lett. 42, 595 (1979).

[7]K. C. Woo and P. J. Stiles, in Proceedings of the IVth International Conference on Electronic Properties of Two-Dimensional Systems (New London, New Hampshire), edited by F. Stern [Surf. Sci. 113, 515 (1982)]; and private communication.

[8]D. C. Tsui and G. Kaminsky, Solid State Commun. 20, 93 (1976).

[9]G. Dorda, H. Gesch, and I. Eisele, Solid State Commun. 20, 429 (1976); G. Dorda, I. Eisele, and H. Gesch, Phys. Rev. B 17, 1785 (1978); G. Dorda, H. Gesch, and I. Eisele, Surf. Sci. 98, 407 (1980); I. Eisele, *ibid.* 73, 315 (1978).

[10]W. L. Bloss, L. J. Sham, and B. Vinter, Phys. Rev. Lett. 43, 1529 (1979).

[11]W. L. Bloss, S. C. Ying, and J. J. Quinn, Phys. Rev. B 23, 1839 (1981).

[12]S. Das Sarma and B. Vinter, Phys. Rev. B 28, 3629 (1983).

[13]B. Vinter and A. W. Overhauser, Phys. Rev. Lett. 44, 47 (1980).

[14]T. Englert, in *Physics in High Magnetic Fields,* Vol. 24 of *Springer Series in Solid State Sciences,* edited by S. Chikazumi and N. Miura (Springer, New York, 1981); K. C. Woo and P. J. Stiles, in Proceedings of the IVth International Conference on Electronic Properties of Two-Dimensional Systems, Ref. 7, p. 278.

[15]M. J. Kelley and L. M. Falicov, Phys. Rev. B 15, 1974 (1977); 15, 1983 (1977).

[16]M. Nakayama, Surf. Sci. 73, 510 (1978).

[17]M. J. Kelly, J. Phys. C 11, 4329 (1978).

[18]G. Beni and T. M. Rice, Phys. Rev. B 20, 5390 (1979).

[19]W. P. Chen, Y. J. Chen, and E. Burstein, Surf. Sci. 58, 263 (1976).

[20]S. J. Allen, D. C. Tsui, and B. Vinter, Solid State Commun. 20, 425 (1976).

[21]T. Ando, Z. Phys. B 26, 263 (1977).

[22]S. Das Sarma, R. K. Kalia, M. Nakayama, and J. J. Quinn, Phys. Rev. B 24, 7181 (1981).

[23]C. S. Ting and A. K. Ganguly, Phys. Rev. B 20, 4244 (1979).

[24]T. Ando, T. Eda, and M. Nakayama, Solid State Commun. 23, 751 (1977).

[25]K. C. Woo and P. J. Stiles, Phys. Rev. B 28, 7101 (1983).

[26]S. M. Nee, V. Claessen, and F. Koch (unpublished).

[27]K. S. Yi and J. J. Quinn, in Proceedings of the IVth International Conference on Electronic Properties of Two-Dimensional Systems, Ref. 7, p. 89.

[28]B. D. McCombe and D. E. Schafer, in *Proceedings of the 14th International Conference of the Physics of Semiconductors, Edinburgh, 1978,* edited by B. L. H. Wilson (IOP, London, 1978), p. 1227.

[29]Previous statements in earlier work (Refs. 30 and 31) to the effect that there was *no* shift between $E_{||}$ and $E_{\perp}$ within experimental error failed to account for the apparently substantial difference in depletion charge among the $E_{\perp}$ and $E_{||}$ samples.

[30]T. Cole and B. D. McCombe, in Proceedings of the 15th International Conference on the Physics of Semiconductors, Kyoto, 1980 [J. Phys. Soc. Jpn. 49, Suppl. A, 959 (1980)].

[31]T. Cole, in Proceedings of the IVth International Conference on the Electronic Properties of Two-Dimensional Systems, Ref. 7, p. 41.